Düzce University Journal of Science & Technology

Research Article

A HRTEM-EDS-SAED Study of Precipitates in Mg-Zn-Zr Alloy

Ozgur DUYGULU [a,*]

[a] *Materials Technologies, TUBITAK MAM, Kocaeli,, TURKEY*
* *Corresponding author's e-mail address: ozgur.duygulu@tubitak.gov.tr*
DOI: 10.29130/dubited.1397327

ABSTRACT

In this study, aging heat treatment was performed on extruded Mg-Zn-Zr alloy. Aging was performed on as-extruded samples at 180°C for 1-2-4-8 and 24 hours. Microhardness tests were made to obtain the aging curve. Detailed transmission electron microscopy (TEM) examinations such as selected area electron diffraction (SAED), energy dispersive spectrometry (EDS), and high resolution transmission electron microscopy (HRTEM) were used to investigate the microstructure, second phases, and precipitates. Size, type, and morphologies of second phases and precipitates were studied aided by advanced transmission electron microscopy techniques. With the help of hardness test results peak aged condition was found to be 8 hour aging. TEM examinations were detailed for the 8-hour aged sample. It was observed that the precipitates responsible for age hardening were $MgZn_2$. Moreover, the majority of these precipitates were β'_1 phase.

Keywords: *TEM, EDS, SAED, Magnesium alloys, Extrusion, Aging*

Mg-Zn-Zr Alaşımında Çökeltilerin HRTEM-EDS-SAED Çalışması

ÖZET

Bu çalışmada, ekstrüde edilmiş Mg-Zn-Zr alaşımına yaşlandırma ısıl işlemi uygulanmıştır. Yaşlandırma, ekstrüzyon sonrası numuneler üzerinde 180°C'de 1-2-4-8 ve 24 saat süreyle gerçekleştirilmiştir. Yaşlanma eğrisinin elde edilmesi için mikrosertlik testleri yapılmıştır. Mikroyapıyı, ikinci fazları ve çökeltileri araştırmak için seçili alan elektron kırınımı (SAED), enerji dağılım spektrometrisi (EDS) ve yüksek çözünürlüklü geçirimli elektron mikroskobu (HRTEM) gibi ayrıntılı geçirimli elektron mikroskobu (TEM) incelemeleri kullanılmıştır. İkinci fazların ve çökeltilerin boyut, tip ve morfolojileri ileri geçirimli elektron mikroskobu teknikleri desteğiyle incelenmiştir. Sertlik sonuçları yardımı ile pik yaşlanma noktasının 8-saat yaşlanma olduğu bulunmuştur. TEM incelemeleri 8-saat yaşlanma numunesinde detaylandırılmıştır. Yaşlanma sertleşmesinden sorumlu çökeltilerin $MgZn_2$ olduğu gözlemlenmiştir. Ayrıca bu çökeltilerin çoğu β'_1 fazıdır.

Anahtar Kelimeler: *TEM, EDS, SAED, Magnezyum alaşımları, Ekstrüzyon, Yaşlandırma*

Received: 28/11/2023, Revised: 02/01/2024, Accepted: 04/04/2024

I. INTRODUCTION

Magnesium alloys, the lightest structural metal alloys, hold significant potential for diverse applications, including automotive, aerospace, defense, and electronic components [1-5]. Traditionally, these parts are mostly made out of cast magnesium alloys. Using wrought magnesium alloys is very limited due to poor cold workability [5]. Another main reason for this is the limited precipitation hardening of wrought magnesium alloys. Wrought magnesium alloys may not match the mechanical properties of wrought aluminum alloys which are precipitation hardenable [4]. Moreover, there are a few industrially available precipitation hardenable magnesium alloys [1-5]. Magnesium-Zinc alloy system is one of the first wrought magnesium alloys that was studied for precipitation hardening. In magnesium alloys zinc element is used for precipitation hardener and increases strength at room temperature [4]. It is also known that magnesium-zinc alloys are generally precipitation-hardened at a temperature range of 120 to 200°C [6]. There are also studies to reduce the aging temperature of these alloys [7]. To understand the age hardening response of Mg-Zn alloys we need to know the phases that are formed during production and the heat treatments.

According to the phase diagram of Mg–Zn, five intermetallic phases are observed: Mg_7Zn_3 (or $Mg_{51}Zn_{20}$), MgZn, Mg_2Zn_3 (or Mg_4Zn_7), $MgZn_2$ and Mg_2Zn_{11} [1-2, 8]. Solubility limit of Zn is 2.4 wt.% (6.2 at.%) [4].

In Mg-Zn alloys eutectic reaction formula is:
L → α-Mg + **Mg_7Zn_3**
The **Mg_7Zn_3** (also known as $Mg_{51}Zn_{20}$) phase is body centered orthorhombic (space group: Immm, a = 1.408 nm, b = 1.449 nm, and c = 1.403 nm). This phase is thermodynamically stable above 598K (325°C) [8-9].

Below and at 598K an eutectoid reaction occurs:
Mg_7Zn_3 → α-Mg + **MgZn**
MgZn intermetallic has base-centered monoclinic crystal structure with lattice parameters: a = 1.610 nm, b = 2.579 nm, c = 0.880 nm and β = 112.4 deg. [8-9].

Below 598K with heat treatments Mg_7Zn_3 may also change to divorced lamellar structure of α-Mg and **Mg_4Zn_7**. Metastable **Mg_4Zn_7** phase is base-centered monoclinic (space group: B/2m, a = 2.596 nm, b = 1.428 nm, c = 0.524 nm and γ = 102.5 deg) [9].

Age hardening of magnesium alloys are generally complex and difficult to understand. Transmission electron microscopy is an unique technique for the investigations of precipitates responsible from age hardening. A series of phase transformations involve in aging of Mg-Zn alloys. The isothermal aging between 120 to 200°C products occur sequentially as:
SSSS Mg → GP zones → β'_1 (**Mg_4Zn_7** or **$MgZn_2$**) → β'_2 (**$MgZn_2$**) → β (MgZn or Mg_2Zn_3) [8-9].

The GP zones generally have two types: GP1 and GP2. GP1 zone plates occur below 60°C on {11-20}. GP2 zones are observed below 80°C as oblate spheroids on (0001) planes. GP zones are known to be coherent [9].

Peak aging forms mainly coherent rod-like β'_1 which grows parallel to $[0001]_\alpha$ or c-axis direction. When the peak aged condition is passed, β'_2 increases in sacrifice of β'_1 with time [10]. β'_1 rods are believed to be typically **Mg_4Zn_7** or **$MgZn_2$**. **$MgZn_2$** is a HCP structure (a = 0.520 nm, c = 0.857 nm). **Mg_4Zn_7** is base-centered monoclinic structure (a = 2.596 nm, b = 1.428 nm, c = 0.524 nm and γ = 102.5 °). Orientation relationship (OR) between β'_1-Mg_4Zn_7 and magnesium matrix is as follows: $[001]_{\beta'1\text{-}Mg4Zn7}$ // $[0001]_\alpha$ and $(630)_{\beta'1\text{-}Mg4Zn7}$ // $(01\text{-}10)_\alpha$ [9]. On the other hand, orientation relationship between β'_1-$MgZn_2$ rod and Mg matrix is $[0001]_{\beta'1\text{-}MgZn2}$ // $[11\text{-}20]_\alpha$ and $(11\text{-}20)_{\beta'1\text{-}MgZn2}$ // $(0001)_\alpha$. [6, 8-9, 11-12].

Semi-coherent β'_2 precipitate is $MgZn_2$ with several shapes and ORs. β'_2 may form as hexagon-shaped parallel to (0001). These are called (0001) plates. OR of these plates is: $(0001)_{\beta'2\text{-}MgZn2}$ // $(0001)_\alpha$ and $[11\text{-}20]_{\beta'2\text{-}MgZn2}$ // $[10\text{-}10]_\alpha$. [9]. Another type of β'_2 - $MgZn_2$ is rod or lath shaped. Orientation relationship between laths and magnesium is $[11\text{-}20]_{\beta'2}$ // $[0001]_\alpha$ and $(0001)_{\beta'2}$ // $(11\text{-}20)_\alpha$ These laths are oriented approximately 6° to {10-10} plane of magnesium matrix [9-11].

Generally, β1' forms as [0001]α rods, whereas the metastable phase β2' forms as (0001)α plates or discs [9, 12]. These rods and plates are given in Figure 1 schematically. It is also found that some plate precipitates may contain both Mg_4Zn_7 and $MgZn_2$ [13].

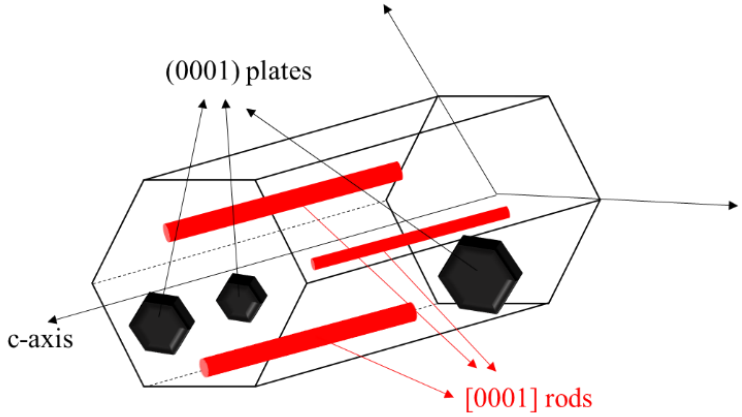

Figure 1. *Schematic representation of [0001] rods and (0001) plates inside magnesium hexagonal prism.*

β (MgZn or Mg_2Zn_3) phase is stated to be incoherent and generally has irregular shapes. It is trigonal (a = 1.724 nm, b = 1.445 nm, c= 0.52 nm and γ = 138°) [14].

Undissolved Mg-Zn(Zr) phase may also be observed. The Mg-Zn(Zr) phase is insensitive to heat treatment and is known to be a stable phase [15].

One of the industrially available commercial Mg-Zn alloy is Mg ZK60 (Mg-5.5Zn-0.5Zr) alloy. The ZK60 alloys has zirconium element which is well known grain refiner [4]. Alloy ZK60 has high strength (340-350 MPa) depending on the production technique and aging condition. It has one of the highest yield strength (285 MPa) among wrought magnesium alloys at ambient temperatures. Additionally this alloy has low tensile-compression asymmetry. Mg ZK60 alloys have good ductility at around 12-16% El. [1-5]. Due to these properties ZK60 magnesium alloys are used for defense applications such as ballistic, aircrafts, helicopters, and personnel carriers [13]. Mg ZK alloys can be produced both by extrusion and also forging methods [1-5].

In this study, commercial Mg ZK60 alloy is studied in the extruded condition. Age hardening response of Mg ZK60 alloy billet was investigated. Detailed transmission electron microscopy techniques were used. The results of this study may be also helpful for other Mg-Zn based alloys such as Mg-Zn-Zr, Mg-Zn-Cu, Mg-Zn-RE, Mg-Zn-Sn, Mg-Zn-Ag, Mg-Zn-Zr-RE, Mg-Zn-Y, Mg-Zn-Y-Ca, Mg-Zn-Ca and Mg-Zn-Ca-RE alloys [16-17].

II. EXPERIMENTAL PROCEDURE

A. PROCESS

In this study, aging heat treatment was performed on extruded Mg-Zn-Zr alloy. Aging was performed on as-extruded samples at 180°C for 1-2-4-8 and 24 hours.

A. 1. Material

Commercial extruded Mg ZK60 Alloy (Mg-5.5Zn-0.5Zr) billet was used. Chemical composition of the Mg ZK60 alloy investigated in the present study is given in Table 1.

Table 1. *Chemical composition of the Mg ZK60 alloy investigated in the present study*.

Zn	Zr	Fe	Si	Cu	Ni
5.52	0.48	0.0120	0.0150	0.0004	0.0001

A. 2. Aging

Aging was performed on as-extruded samples. Aging temperature was chosen as 180°C and aging times were 1-2-4-8 and 24 hours.

B. CHARACTERIZATION

B. 1. Microhardness Test

Vickers microhardness measurements were performed with a 5 kg applied load with a Qness Q10 A+ device. For each sample hardness values were calculated from average of 5 test readings.

B. 2. Transmission Electron Microcsopy

For transmission electron microscopy (TEM) studies, specimens were cut to a thickness of around 300 µm with Struers Minitom low speed diamond saw. 3 mm diameter discs were punched and ground to a thickness less than 80 µm. Punched specimens were dimple ground with Gatan 656 Dimple Grinder. The center of the specimen was thinned down to 15 µm. Specimens were ion milled with Gatan 691 Precision Ion Polishing System (PIPS). Ion polishing was applied first at 5 kV at an angle of ±8° and when it was perforated at 4kV, 3kV and finally at 2kV at an angle of ±8° for 1-2 hours each.

The foils were examined with a JEOL JEM 2100 HRTEM (high resolution transmission electron microscope) with a LaB_6 filament operated at 200 kV and equipped with an Oxford Instruments X-MaxN 80 T with Energy Dispersive Spectrometry (EDS) system. TEM and diffraction patterns were imaged with Gatan Model 833 Orius SC200D CCD side Camera. HRTEM images were taken by Gatan Model Model 794 Slow Scan CCD Camera. JEOL 31630 side entry double tilt holder and JEOL 21010 single tilt holder were used.

TEM Dark Field (DF), Bright Field (BF), Selected Area Electron Diffraction (SAED), HRTEM and Energy Dispersive Spectrometry (EDS) techniques were used to investigate the microstructure. Gatan Microscopy Suite 2 software analyzed the images. EDS analysis was performed by Oxford INCA software. For diffraction pattern analysis and crystallography purposes CrystBox software was used [18]. For crystallography and d-spacing calculations ICSD (Inorganic Crystal Structure Database) PDF numbers were 35-821 for Mg, 34-0457 for $MgZn_2$ and 01-1185 for Mg_4Zn_7.

III. RESULTS AND DISCUSSIONS

Age hardening curve was plotted (Figure 2) from the microhardness test results. It was observed that hardness increased from as-extruded value of 68 HV to a peak aging value of 72.5 HV at around 8 hour. This corresponds to 6.6% increase. Than hardness decreased to 70.5 HV at 24 hour. Therefore 8 hour can be named as peak aged and 24 hour as over-aged condition. Since in this study the aim is to understand hardening behavior of Mg ZK60 alloy, 8 hour (peak aged) sample was chosen for detailed transmission electron microscopy investigations.

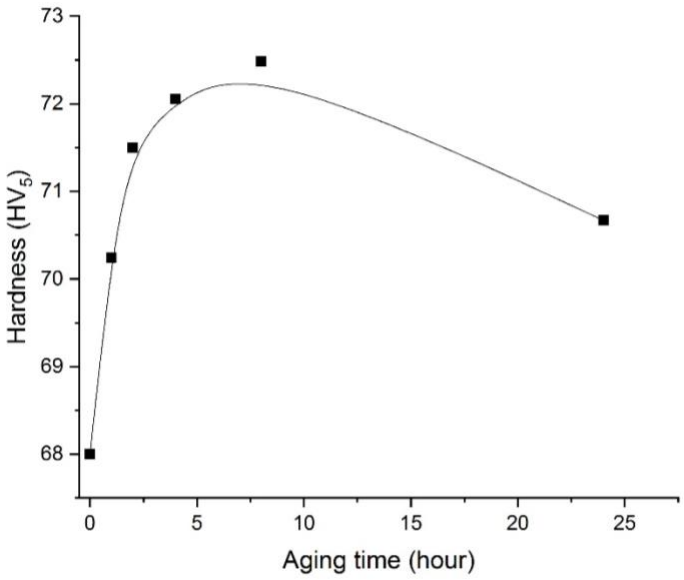

Figure 2. *Age hardening curve of Mg ZK60 alloy at 180°C.*

Transmission electron microscopy investigations were first performed on the starting material which is as-extruded specimens. As-extruded sample had sub-micron second phases. In Figure 3 TEM image, TEM-EDS spectrum and EDS results of agglomeration of sub-micron second phases in as-extruded sample are given. TEM-EDS showed high amount of zinc element and some zirconium element. In the background some precipitates are also seen.

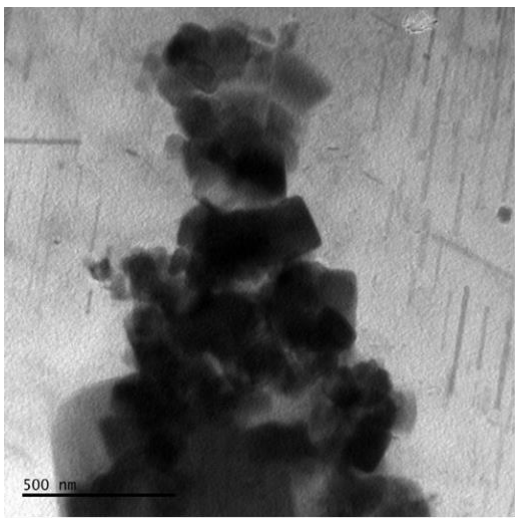

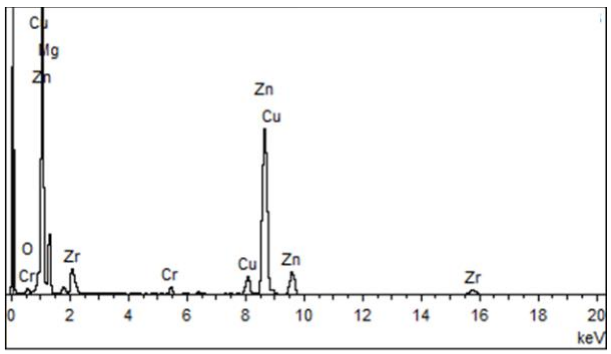

Element	Weight%	Atomic%
Mg	10.94	25.41
Zn	79.34	68.57
Zr	9.72	6.02

Figure 3. *Transmission electron microscopy image, TEM-EDS spectrum and EDS results of agglomeration of sub-micron second phases in Mg ZK60 as-extruded sample.*

Detailed TEM examinations on peak aged sample showed different kinds of second phases. First type of second phases was sub-micron sized and irregular shaped particles. Low magnification transmission electron microscopy image and corresponding TEM-EDS spectrum and EDS results of sub-micron second phases in 8-hour sample are given in Figure 4. These particles are observed on the grain boundary. Since TEM-EDS gave Mg-Zn elements these particles can be called as "blocky" $MgZn_2$ type particles. Similar particles were also observed by several researchers [6, 7, 14, 15, 19]. In Figure 4, on the left side of the grain boundary a high density of rod shaped up to 200 nm length precipitates are also observed.

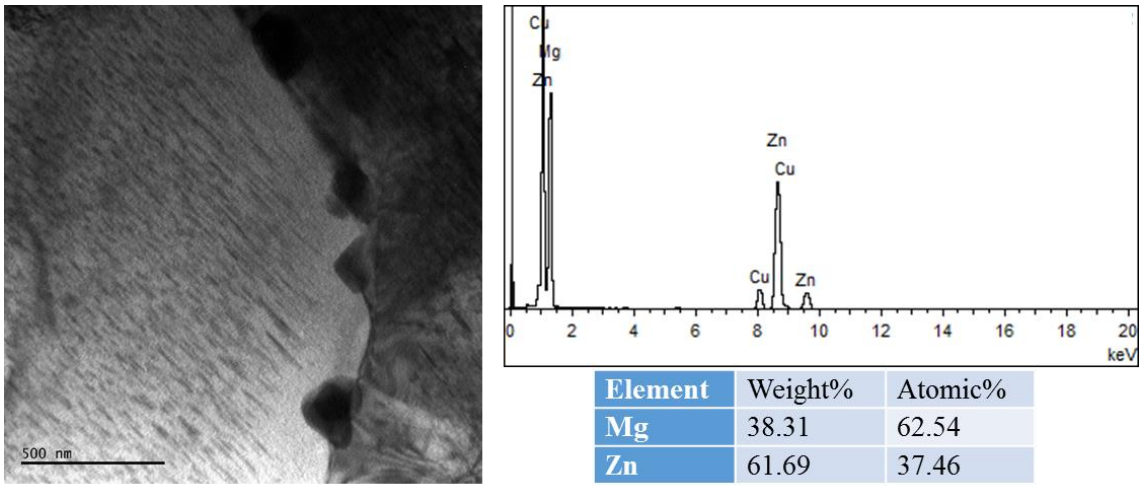

Element	Weight%	Atomic%
Mg	38.31	62.54
Zn	61.69	37.46

Figure 4. *TEM image, TEM-EDS spectrum and EDS results of sub-micron second phases in 8-hour sample.*

Another low magnification TEM image is given in Figure 5 for the peak-aged sample. Here rod type precipitates oriented parallel to [0002] axis of magnesium are seen clearly. Length of some of these precipitates are as high as 1 µm. Other than general observation of the microstructure, in this Figure a few plate type precipitates (inside white circles) perpendicular to [0002] direction were also found. It can be stated that rod type precipitates are β'_1 - $MgZn_2$ and perpendicular plates are β'_2 - $MgZn_2$. To see both type of precipitates is more common in over aged samples where size and number of the plate type precipitates increases and become extensive [6,9,10]. However in some studies observation of both rods and plates at the same time at the peak aged Mg-Zn alloys was also possible [10,14].

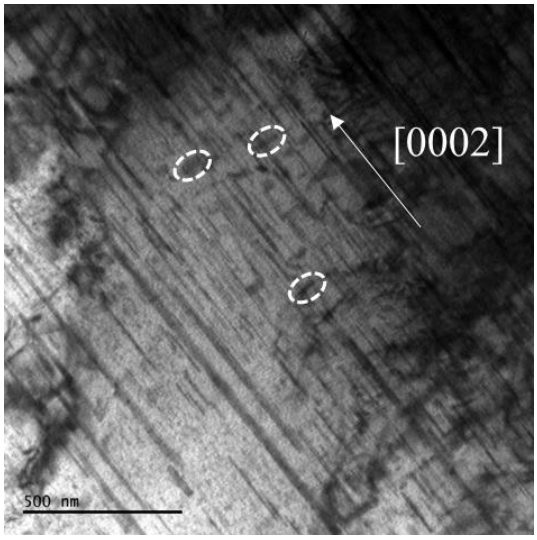

Figure 5. *Rod type precipitates oriented parallel to [0002] axis of magnesium and plate type precipitates (inside white circles) perpendicular direction in peak aged sample.*

Rod type precipitates oriented parallel to [0002] axis of magnesium were also observed in another part of the 8-hour TEM sample. Corresponding SAED, indexation for magnesium matrix, and hexagonal prism directions of magnesium and $MgZn_2$ precipitates were also given in Figure 6. The SAED indexation and directions were performed with the help of CrystBox software [18]. In the diffraction pattern the spots inside blue circles gave a d-spacing of 0.21 nm which matches pretty good with d-0004 of $MgZn_2$. It is found that zone axis of the SAED is [-7253] of Mg. Even if it is a high index zone axis, it was possible to get the directions of hexagonal prisms of magnesium and $MgZn_2$ precipitates. [0002] directions or c-axis of magnesium and $MgZn_2$ are perpendicular to each other. Since all precipitates are oriented in one direction, it can be stated that there is only a single phase. It is known that orientation relationship between β'_1 - $MgZn_2$ rod and Mg matrix is $[0001]_{\beta'1\text{-}MgZn2}$ // $[11\text{-}20]_{\alpha}$. [6,8,9,111]. In our case since c-axis of magnesium is perpendicular to c-axis of $MgZn_2$ this given orientation relationship is matched. Therefore these precipitates are most probably β'_1 - $MgZn_2$ rods.

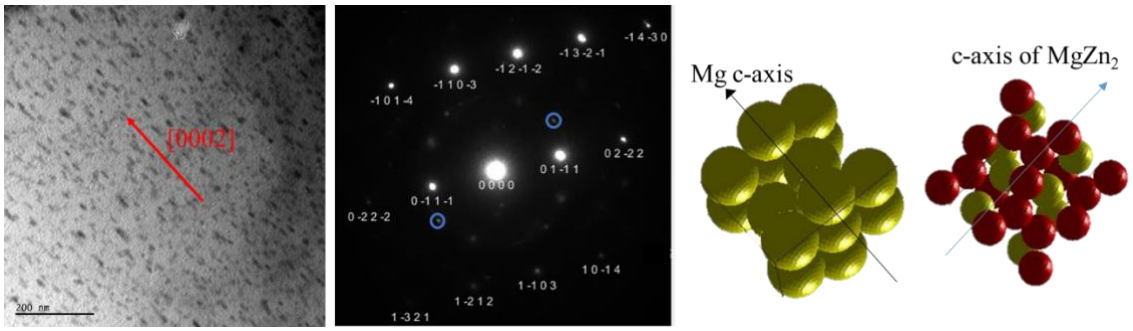

Figure 6. *TEM image of rod type precipitates, corresponding SAED and hexagonal prism directions of magnesium and $MgZn_2$ precipitates in 8-hour TEM sample.*

In Figure 7, TEM image, TEM-EDS spectrum and EDS results of rod shaped precipitate as shown inside red circle in peak-aged sample are given. Since one of the large precipitate was chosen for nano analysis high counts could be achieved. TEM-EDS gave Zr addition to Zn element. Most studies were performed on Mg-Zn alloys; and TEM, HRTEM or SAED techniques were used. There is very limited TEM-EDS studies on Mg-Zn-Zr alloys. EDS were mostly done on larger particles. Therefore, to our knowledge observation of Zr element in the nano sized rod type precipitates of Mg-Zn-Zr alloy is missing in the literature.

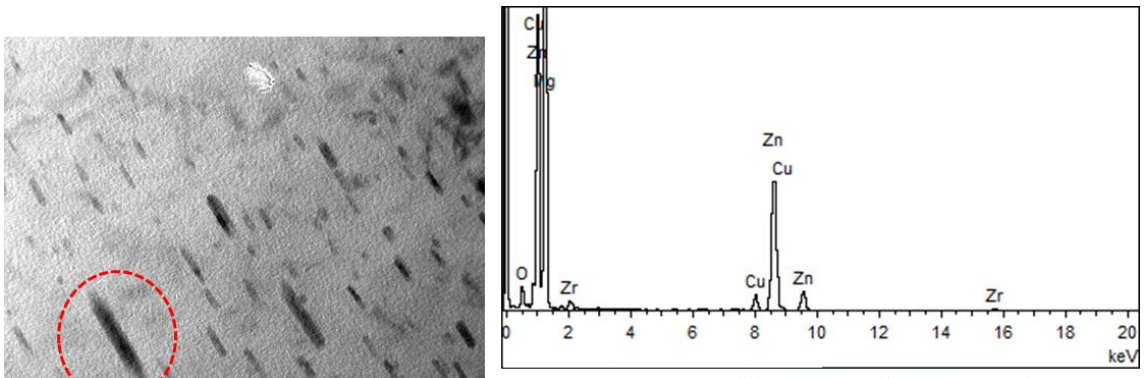

Element	Weight%	Atomic%
Mg	60.29	80.62
Zn	37.09	18.45
Zr	2.62	0.93

Figure 7. *TEM image, TEM-EDS spectrum and EDS results of rod shaped precipitate as shown inside red circle in peak-aged sample.*

HRTEM images, FFT (Fast Fourier Transformation) of HRTEM image and d-spacing measurements of the precipitate red circled in Figure 7 are given in Figure 8. Measurements were done with the help of Gatan Microscopy Suite (GMS) 2 software. The measured d-spacing from both atomic lattice and FFT was 0.43 nm which was a good match with $MgZn_2$ phase. It can be said that zirconium element in the rod type precipitate does not change the d-spacing of $MgZn_2$ significantly.

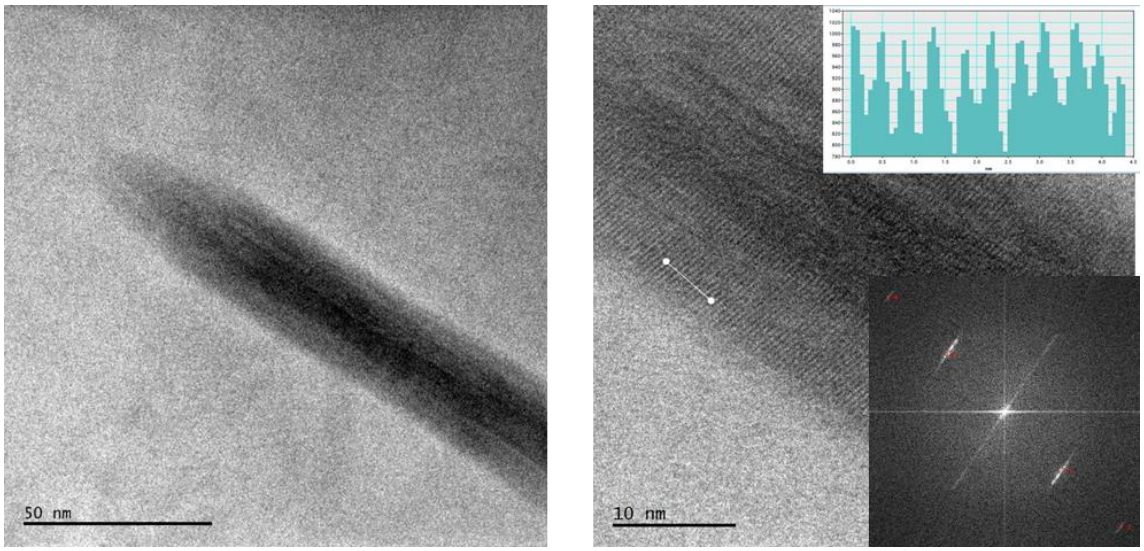

Figure 8. *HRTEM images, FFT image and d-spacing measurements of the circled precipitate in Figure 7.*

IV. CONCLUSIONS

In this study, the hardening behavior of extruded Mg ZK60 (Mg-5.5Zn-0.5Zr) alloy was studied. From the hardening curve obtained with the hardness test, 8-hour (peak aged) sample was chosen for detailed transmission electron microscopy investigations. TEM examinations performed were selected area electron diffraction (SAED), energy dispersive spectrometry (EDS), and high resolution transmission electron microscopy (HRTEM).

Several types, sizes, and morphology of second phases were observed during TEM-EDS-SAED examinations. Sub-micron second phase particles containing Zn and Zr elements were found in the Mg ZK60 as-extruded sample. In the peak-aged sample "blocky" $MgZn_2$-type particles were also seen at some grain boundaries. The dominant phase was rod-type precipitates oriented parallel to [0002] axis of the magnesium matrix. It is stated that these rod-type precipitates are β'_1 - $MgZn_2$ phase responsible for hardening. In rare places, β'_2 - $MgZn_2$ phase were also observed as plates or discs especially perpendicular to β'_1 - $MgZn_2$ rods.

High resolution transmission electron microscopy (HRTEM) investigations on rod type precipitates showed that the measured d-spacing from both atomic lattice and FFT was a good match with $MgZn_2$ phase. Since it was possible to get energy dispersive spectrometry (EDS) results on that specific precipitate and Zr element is found, it can be concluded that the precipitates observed in Mg-Zn-Zr alloys may have not only Mg-Zn precipitates, but also Mg-Zn-Zr precipitates.

V. REFERENCES

[1] M. M. Avedesian, and H. Baker, *Magnesium and magnesium alloys, ASM Specialty Handbook*, Ohio, 1999.

[2] E.F. Emley, *Principles of magnesium technology*, Pergamon, Oxford, 1966.

[3] H. E. Friedrich and B. L. Mordike, *Magnesium technology*, Vol. 212, Springer-Verlag Berlin Heidelberg, 2006.

[4] I. J. Polmear, *Light alloys, metallurgy of the light elements*, Arnold, London, 2006.

[5] K.U. Kainer and F. V. Buch, *The current state of technology and potential for further development of magnesium applications, Magnesium Alloys and Technology*, Wiley-VCH, 2003.

[6] X. Gao and J. F. Nie, "Characterization of strengthening precipitate phases in a Mg–Zn alloy," Scr. Mater., vol. 56, no. 8, pp. 645–648, 2007.

[7] J. Buha, "Reduced temperature (22-100 °C) ageing of an Mg-Zn alloy," *Mater. Sci. Eng. A*, vol. 492, no. 1–2, pp. 11–19, 2008.

[8] X. Gao and J. F. Nie, "Structure and thermal stability of primary intermetallic particles in an Mg-Zn casting alloy," Scr. Mater., vol. 57, no. 7, pp. 655–658, 2007.

[9] J. F. Nie, "Precipitation and hardening in magnesium alloys," *Metall. Mater. Trans. A Phys. Metall. Mater. Sci.*, vol. 43, no. 11, pp. 3891–3939, 2012.

[10] L. Y. Wei, G. L. Dunlop, and H. Westengen, "Precipitation Hardening of Mg-Zn and Mg-Zn-RE alloys," *Metall. Mater. Trans. A*, vol. 26, no. 7, pp. 1705–1716, 1995.

[11] Z. Z. Shi, H. T. Chen, K. Zhang, F. Z. Dai, and X. F. Liu, "Crystallography of precipitates in Mg alloys," *J. Magnes. Alloy.*, vol. 9, no. 2, pp. 416–431, 2021.

[12] Y. Yang, S. Yang, and L. Jiang, "Study on the microstructural characteristics of adiabatic shear band in solid-solution treated ZK60 magnesium alloy," *Mater. Charact.*, vol. 156, no. July, p. 109840, 2019.

[13] H. Chen, T. Liu, Y. Zhang, B. Song, D. Hou, and F. Pan, "The yield asymmetry and precipitation behavior of pre-twinned ZK60 alloy," *Mater. Sci. Eng. A*, vol. 652, pp. 167–174, 2016.

[14] Y. Yang, Z. Wang, and L. Jiang, "Evolution of precipitates in ZK60 magnesium alloy during high strain rate deformation," *J. Alloys Compd.*, vol. 705, pp. 566–571, 2017.

[15] Z. Wang *et al.*, "Effect of aging-treatment on dynamic compression behaviour and microstructure of ZK60 alloy," *Mater. Sci. Technol. (United Kingdom)*, vol. 37, no. 13, pp. 1117–1128, 2021.

[16] A. Gorny and A. Katsman, "Precipitation- and stress-influenced coarsening in Mg-based Mg-Zn-Sn-Y and Mg-Zn-Sn-Sb alloys," J. Mater. Res., vol. 23, no. 5, pp. 1228–1236, 2008.

[17] C. Hou *et al.*, "Aging hardening and precipitate behavior of a solution-treated Mg-6Zn-4Sn-1Mn (wt.%) wrought Mg alloy," *J. Alloys Compd.*, vol. 889, p. 161640, 2022.

[18] M. Klinger. CrysTBox - Crystallographic Toolbox. Institute of Physics of the Czech Academy of Sciences, Prague, 2015. ISBN 978-80-905962-3-8. URL http://www.fzu.cz/~klinger/ crystbox.pdf

[19] J. Tang, L. Chen, Z. Li, G. Zhao, and C. Zhang, “Formation of abnormal coarse grains and its effects on corrosion behaviors of solution treated ZK60 Mg alloy,” Corros. Sci., vol. 180, no. September 2020, p. 109201, 2021.